Supplemental Results

Measurement of Ca^{2+} responses after DHPG stimulation.

DHPG alone (100 μM) elicited no increase in intracellular Ca^{2+} levels under control conditions in the majority of WT PCs, as measured by fura-2. This situation is common to other neuronal cell types in culture and is explained by the fact that in resting conditions, primary neurons in culture can have empty stores, so that DHPG alone is not able to elicit a Ca^{2+} response (1). To overcome this problem, we applied a moderate depolarization (two pulses of KCl at submaximal concentration (6 mM) in order to fill the stores), and then treated PCs with 100 μM DHPG. DHPG is specific for the group I mGluR, which includes mGluR5 and mGluR1. It is well established from the literature that mature PCs express only mGluR1 (2). However, little is known about the expression of mGluR5 in primary PCs in culture. We therefore performed IF on primary PCs using Ab against mGluR1 and calbindin or mGluR5 and calbindin, which revealed expression of both receptors in PCs in this time window (Supplemental Figure 8A and B). For this reason, we decided to pre-treat PCs with the selective mGluR5 antagonist 2-methyl-6-(phenylethynyl) pyridine (MPEP) (10 μM) before eliciting the DHPG response. In this condition, after DHPG stimulation we could detect a Ca^{2+} response in WT cells, which was absent in *Grm1* $^{crv4/crv4}$ PCs, demonstrating that inactivation of mGluR1 in PCs abolishes ER-mediated Ca^{2+} responses (Supplemental Figure 3, A and B).

Supplemental Methods

Ab, drugs and reagents.

For WB, commercially available monoclonal Ab were used for the detection of mouse anti-mGluR1 (M2620-050 BD biosciences, Franklin Lakes, NJ, USA); mouse anti-GluR1-NT clone RH95 (Millipore), β-tubulin (E7, Developmental Studies Hybridoma Bank, University of Iowa, USA).

For IF experiments the following Ab were used: mouse anti-mGluR1 (M2620-050 BD biosciences); mouse anti-mGluR5 (2237-1Epitomics, Burlingame, CA, USA).

For fura-2 measurement of Ca^{2+} levels the following reagents were used: 2-methyl-6-(phenylethynyl) pyridine hydrochloride (MPEP, Tocris) and (S)-3,5-dihydroxyphenylglycine (DHPG, Tocris).

Spectrophotometric assay of Complex I activity.

Complex I enzymatic activity was measured as described previously (3) with slight modifications.

The enzymatic activity of complex I was assayed spectrophotometrically and the result was normalized to the activity of citrate synthase. This protocol was applied on frozen cerebella derived from 12 mo old mice. Tissues were weighed, diluted 1:9 in ice-cold sucrose homogenization buffer (20 mM Tris-HCl pH 7.4, 40 mM KCl, 2 mM EGTA, 250 mM sucrose) and homogenized using a glass-Teflon homogenizer. Cell debris was discarded by centrifugation at 600 *g* for 10 min at 4°C. For complex I activity, 120 µg of cerebellar proteins were resuspended in 0.5 M potassium phosphate buffer pH 7.5 (0.5 M potassium phosphate dibasic with 0.5 M potassium phosphate monobasic), 50 mg/ml BSA (Sigma), 100 µM sodium azide (Sigma), 100 µM NADH (Sigma). The reaction was stimulated with 60 µM ubiquinone (Sigma). Samples treated with 10 µm rotenone (Sigma) were used as negative controls. The activity of complex I was evaluated by measuring the decrease of absorbance at 340 nm for 2 min.

For citrate synthase activity 27 µg of cerebellar proteins were resuspended in 200 mM Tris-HCl pH 8.0 with 0.2% Triton X-100, 100 µM 5-5'-dithiobis(2-nitrobenzoic acid) (DTNB; Sigma), 0.3 mM Acetyl CoA lithium salt (Sigma). The reaction was stimulated with 0.5 mM oxalacetic acid (Sigma). The activity of citrate synthase was evaluated by measuring the increase of absorbance at 412 nm for 2 min. Data represent the ratio between complex I activity and citrate synthase activity.

Supplemental Figure legends.

Supplemental Figure 1. Immunofluorescence on cerebellar slices of *Afg3l2*$^{+/+}$, *Afg3l2*$^{+/-}$ and *Afg3l2*$^{-/-}$ mice without AMPA treatment at 10 post-natal days using an Ab against calbindin (PC marker, green) and Ab against SBDP (spectrin break down products, red).

Supplemental Figure 2. (A) Immunofluorescence on PC culture *Afg3l2*$^{+/+}$ at 14 DIV using Ab against calbindin (PCs marker, green), GFAP (astrocytes marker, red), NeuN (neuronal marker, red) and mGluR1. Pictures acquired by confocal microscopy. (B-D) Quantification of: the number of dendrites (B), the length of the longest dendrite (C) and spine density (D). Means ± SD, n=6, an average of 20 neurons analyzed per genotype/experiment. Student's *t* test: *p< 0.05.

Supplemental Figure 3. (A and B) Representative traces of $[Ca^{2+}]_c$ in a single PCs of *Grm1*$^{+/+}$ and *Grm1*$^{crv4/crv4}$, showing lack of Ca^{2+} responses in the absence of mGluR1. PCs were pre-treated with the selective mGluR5 antagonist MPEP before eliciting the Ca^{2+} response with DHPG, a specific group I mGluR agonist. (C) Means ± SEM of $[Ca^{2+}]_c$ peak responses after 100 μM DHPG stimulation normalized to Ca^{2+} peak responses after 6 mM KCl stimulation. An average of 35 traces per genotype from three independent experiments was analyzed. Student's *t* test: **p<0.001, *p<0.05.

Supplemental Figure 4. (A) WB analysis on cerebellar extracts from *Grm1*$^{+/+}$ and *Grm1*$^{+/crv4}$ using anti-mGluR1 Ab. β-tubulin was used to verify equal loading. (B) WB analysis on cerebellar extracts from *Afg3l2*$^{+/-}$ *Grm1*$^{+/crv4}$ mice and littermates of the indicated genotypes using anti-AMPA receptor subunits1 (GluR1-NT) Ab. β-tubulin was used to verify equal loading.
(C) Representative pictures of semithin sections of *Grm1*$^{+/+}$ and *Grm1*$^{+/crv4}$ mice at 3 mo (left) and 8 mo (right), revealing no signs of degeneration in the mutants compared to controls. (D) Quantification of healthy and dark PCs in *Grm1*$^{+/+}$ and *Grm1*$^{+/crv4}$ at 3 and 8 mo. Bars represent means ± SD, n=3. (E) Cryostat sections of cerebellum of *Afg3l2*$^{+/-}$ *Grm1*$^{+/crv4}$ mice and littermates at 12 mo stained with anti-calbindin and anti-mGluR5 Ab, revealing the complete absence of mGluR5 in adult PCs.

Supplemental Figure 5. (A) WB showing increased expression of EAAT2 in ceftriaxone-treated *Afg3l2*$^{+/-}$ mice compared to controls (synaptosomal fractions from cerebellum) after 8 weeks from treatment. Post-synaptic density 95 kDa protein (PSD95) was used to verify equal loading. v = vehicle, cef = ceftriaxone. (B) Cryostat sections stained with anti-calbindin Ab of *Afg3l2*$^{+/+}$ mice treated with vehicle or ceftriaxone

Supplemental Figure 6. (A) Ultrathin section of cerebellum from *Afg3l2*$^{+/-}$ *Grm1*$^{+/+}$ and *Afg3l2*$^{+/-}$ *Grm1*$^{+/crv4}$ at 12 mo. (B) Quantification of mitochondrial ultrastructural alterations. The organelles were classified as normal, vesicular and swollen on basis of inner membrane remodeling. The graphs indicate means ± SD of an average of 1000 mitochondria coming from 15 cells per mouse (n=3 per genotype, at least). Chi squared test was applied for significance calculation (degrees of freedom = 2, WT versus either *Afg3l2*$^{+/-}$ *Grm1*$^{+/+}$ or *Afg3l2*$^{+/-}$ *Grm1*$^{+/crv4}$ $^{**}p<0.001$). (C) Ultrathin section of cerebellum from *Afg3l2*$^{+/-}$ mice treated with vehicle or ceftriaxone at 12 mo. (D) Quantification of mitochondrial ultrastructural alteration. The graphs indicate means ± SD of an average of 1000 mitochondria coming from 15 cells per mouse (n=3 per genotype, at least). (E) EM on primary PCs of *Afg3l2*$^{-/-}$ *Grm1*$^{+/+}$ and *Afg3l2*$^{-/-}$ *Grm1*$^{+/crv4}$ treated with either vehicle or DHPG at 10 DIV, showing the presence of aberrant mitochondria in both genotypes and both experimental conditions.

Supplemental Figure 7. (A) Graphs show means ± SD of complex I activity normalized to citrate synthase activity (spectrophotometric assay of cerebellar homogenates from *Afg3l2*$^{+/-}$ *Grm1*$^{+/crv4}$ and littermates at 12 mo, n=3). (B) Means ± SD of complex I activity normalized to citrate synthase activity (spectrophotometric assay of cerebellar homogenates from *Afg3l2*$^{+/-}$ and WT treated with vehicle and ceftriaxone at 12 mo, n=3).

Supplementary Figure 8. (A) IF on primary PCs of the indicated genotypes at 10 DIV using Ab against the PC marker calbindin and the metabotropic glutamate receptor 5 (mGluR5). (B) IF on primary PCs of the indicated genotypes at 10 DIV using Ab against the PC marker calbindin and the metabotropic glutamate receptor 1 (mGluR1). These analyses revealed expression of both receptors in primary PCs at 10 DIV.

Supplemental Table 1

SHIRPA test to evaluate sensory and motor functions of *Afg3l2*$^{+/-}$*Grm1*$^{+/+}$, *Afg3l2*$^{+/-}$*Grm1*$^{+/crv4}$, *Afg3l2*$^{+/+}$*Grm1*$^{+/+}$ and *Afg3l2*$^{+/+}$*Grm1*$^{+/crv4}$ mice (n=10). Data are expressed as mean ± SD (Mann-Whitney non-parametric test; ** for "gait" $p<0.001$ is referred to *Afg3l2*$^{+/-}$*Grm1*$^{+/+}$ versus *Afg3l2*$^{+/-}$*Grm1*$^{+/crv4}$, *Afg3l2*$^{+/+}$*Grm1*$^{+/+}$ and *Afg3l2*$^{+/+}$*Grm1*$^{+/crv4}$; ** for "negative geotaxis" $p<0.001$ is referred to *Afg3l2*$^{+/-}$*Grm1*$^{+/+}$ versus *Afg3l2*$^{+/+}$*Grm1*$^{+/+}$ and *Afg3l2*$^{+/+}$*Grm1*$^{+/crv4}$).

Genotype / Behavior	*Afg3l2*$^{+/+}$*Grm1*$^{+/+}$	*Afg3l2*$^{+/+}$*Grm1*$^{+/crv4}$	*Afg3l2*$^{+/-}$*Grm1*$^{+/+}$	*Afg3l2*$^{+/-}$*Grm1*$^{+/crv4}$
Body position	3 ± 0	3 ± 0	3 ± 0	2,7 ± 0,8
Spontaneous activity	2,2 ± 0,7	2 ± 0	2 ± 0	2 ± 0,8
Respiration	2 ± 0	2 ± 0	2 ± 0	2 ± 0
Tremor	0 ± 0	0 ± 0	0 ± 0	0 ± 0
Transfer arousal	4 ± 0,7	3,9 ± 0,5	3,4 ± 1,1	3 ± 1,1
Palpebral closure	0 ± 0	0 ± 0	0 ± 0	0 ± 0
Piloerection	0,13 ± 0,35	0 ± 0	0,2 ± 0,4	0,2 ± 0,4
Startle response	0,9 ± 0,8	0,6 ± 0,5	0,4 ± 0,5	0,5 ± 0,5
Gait	0 ± 0	0 ± 0	0,4 ± 0,5**	0,3 ± 0,8
Pelvic elevation	2,1 ± 0,3	2 ± 0	2,2 ± 0,4	1,8 ± 0,5
Tail elevation	0,1 ± 0,3	0 ± 0	0,4 ± 0,5	0 ± 0
Touch escape	0,8 ± 0,8	1 ± 0,4	0,8 ± 1	0,5 ± 0,6
Positional passivity	1,7 ± 0,5	1,8 ± 0,4	2 ± 0	1,8 ± 0,7
Pinna reflex	0,2 ± 0,4	0,2 ± 0,4	0,2 ± 0,4	0,2 ± 0,4
Corneal reflex	1 ± 0	1 ± 0	1 ± 0	0,9 ± 0,2
Toe pinch	0,8 ± 0,6	1,1 ± 0,7	0,6 ± 0,5	0,8 ± 0,5
Limb grasping	1 ± 0	1 ± 0	1 ± 0	1 ± 0
Visual placing	3 ± 0	3 ± 0	3 ± 0	3 ± 0
Grip strength	1,6 ± 0,7	2 ± 0,5	1,8 ± 0,5	1,8 ± 0,5
Body tone	0 ± 0	0 ± 0	0 ± 0	0 ± 0
Heart rate	1,5 ± 0,5	1,3 ± 0,4	1,6 ± 0,5	1,6 ± 0,5
Limb tone	0 ± 0	0 ± 0	0 ± 0	0,25 ± 0,8
Abdominal tone	0 ± 0	0 ± 0	0 ± 0	0 ± 0
Lacrimation	0 ± 0	0 ± 0	0 ± 0	0 ± 0
Salivation	0 ± 0	0 ± 0	0 ± 0	0 ± 0
Provoked biting	0,5 ± 0,5	0,9 ± 0,3	0,8 ± 0,4	0,8 ± 0,4
Righting reflex	1 ± 0	1 ± 0	1 ± 0	1 ± 0
Negative geotaxis	0 ± 0	0 ± 0	1 ± 0,8**	1 ± 1,5
Fear	0 ± 0	0 ± 0	0 ± 0	0 ± 0
Irritability	0,8 ± 0,3	1 ± 0	1 ± 0	1 ± 0
Aggression	0,5 ± 0,5	0,5 ± 0,5	0,8 ± 0,4	0,4 ± 0,5
Vocalization	0 ± 0	0 ± 0	0 ± 0	0 ± 0

Table S2

SHIRPA test on *Afg3l2*$^{+/-}$ and *Afg3l2*$^{+/+}$ mice treated with either vehicle or ceftriaxone (n=10). Data are expressed as mean ± SD (Mann-Whitney non-parametric test; for "gait " ** p<0.001 is referred to *Afg3l2*$^{+/-}$ mice-vehicle versus (i) *Afg3l2*$^{+/-}$ mice-ceftriaxone, (ii) *Afg3l2*$^{+/+}$ mice-vehicle and (iii) *Afg3l2*$^{+/+}$ mice-ceftriaxone; for "negative geotaxis" ** p<0.001 is referred to *Afg3l2*$^{+/-}$ mice-vehicle versus (i) *Afg3l2*$^{+/+}$ mice-vehicle and (ii) *Afg3l2*$^{+/+}$ mice-ceftriaxone.

Genotype / **Behavior**	*Afg3l2*$^{+/+}$ vehicle	*Afg3l2*$^{+/+}$ ceftriaxone	*Afg3l2*$^{+/-}$ vehicle	*Afg3l2*$^{+/-}$ ceftriaxone
Body position	3 ± 0	3 ± 0	3 ± 0	3 ± 0
Spontaneous activity	2 ± 0	2 ± 0	2 ± 0	2 ± 0
Respiration	2 ± 0	2 ± 0	2 ± 0	2 ± 0
Tremor	0 ± 0	0 ± 0	0,1 ± 0,3	0 ± 0
Transfer arousal	3 ± 1,2	3,3 ± 1,1	3,2 ± 1,2	3,7 ± 1,5
Palpebral closure	0 ± 0	0 ± 0	0 ± 0	0 ± 0
Piloerection	0,13 ± 0,35	0,2 ± 0,4	0,2 ± 0,4	0 ± 0
Startle response	1,1 ± 0,6	0,8 ± 0,8	1,5 ± 0,8	0,7 ± 0,5
Gait	0,1 ± 0,4	0 ± 0	0,9 ± 0,3**	0,3 ± 0,5
Pelvic elevation	2 ± 0	2 ± 0	2 ± 0	2,1 ± 0,4
Tail elevation	0,1 ± 0,3	0 ± 0	0 ± 0	0,3 ± 0,5
Touch escape	1,8 ± 0,7	1,6 ± 0,5	1,8 ± 0,8	0,9 ± 0,9
Positional passivity	1,4 ± 0,7	1,6 ± 0,5	1,5 ± 0,5	1,4 ± 0,9
Pinna reflex	0 ± 0	0,2 ± 0,4	0,3 ± 0,5	0 ± 0
Corneal reflex	1 ± 0	1 ± 0	1 ± 0	1 ± 0
Toe pinch	1,6 ± 1,2	2,2 ± 1,1	1,6 ± 1	2,1 ± 0,9
Limb grasping	0,9 ± 0,4	1 ± 0	0,9 ± 0,3	1 ± 0
Visual placing	3 ± 0	3 ± 0	3 ± 0	3 ± 0
Grip strength	1,9 ± 0,4	2 ± 0	1,8 ± 0,4	1,6 ± 0,3
Body tone	0 ± 0	0 ± 0	0 ± 0	0 ± 0
Heart rate	1,3 ± 0,5	1,4 ± 0,4	1,4 ± 0,5	1,1 ± 0,5
Limb tone	0 ± 0	0 ± 0	0 ± 0	0,25 ± 0,8
Abdominal tone	0 ± 0	0 ± 0	0 ± 0	0 ± 0
Lacrimation	0 ± 0	0 ± 0	0 ± 0	0 ± 0
Salivation	0 ± 0	0 ± 0	0 ± 0	0 ± 0
Provoked biting	0,9 ± 0,4	0,6 ± 0,5	0,7 ± 0,5	0,7 ± 0,5
Righting reflex	1 ± 0	1 ± 0	1 ± 0	1 ± 0
Negative geotaxis	0,5 ± 0,4	0,4 ± 0,5	1,4 ± 0,6**	0,9 ± 0,5
Fear	0 ± 0	0 ± 0	0 ± 0	0 ± 0
Irritability	0,5 ± 0,5	0,4 ± 0,5	0,6 ± 0,5	0,7 ± 0,5
Aggression	0,8 ± 0,5	0,4 ± 0,5	0,3 ± 0,4	0,6 ± 0,5
Vocalization	0 ± 0	0 ± 0	0 ± 0	0 ± 0

Video

Video 1: Beam-walking test on *Afg3l2*$^{+/-}$ *Grm1*$^{+/+}$ at 8 mo.

Video 2: Beam-walking test on *Afg3l2*$^{+/-}$ *Grm1*$^{+/crv4}$ at 8 mo.

Video 3: Beam-walking test on presymptomatic *Afg3l2*$^{+/-}$ mice treated with vehicle. Age at test: 8 mo.

Video 4: Beam-walking test on presymptomatic *Afg3l2*$^{+/-}$ mice treated with ceftriaxone. Age at test: 8 mo.

Video 5: Beam-walking test on postsymptomatic *Afg3l2*$^{+/-}$ mice treated with vehicle. Age at test: 12 mo.

Video 6: Beam-walking test on postsymptomatic *Afg3l2*$^{+/-}$ mice treated with ceftriaxone. Age at test: 12 mo.

Supplemental references

1. Rae, M.G., Martin, D.J., Collingridge, G.L., and Irving, A.J. 2000. Role of Ca2+ stores in metabotropic L-glutamate receptor-mediated supralinear Ca2+ signaling in rat hippocampal neurons. *J Neurosci* 20:8628-8636.
2. Ferraguti, F., and Shigemoto, R. 2006. Metabotropic glutamate receptors. *Cell Tissue Res* 326:483-504.
3. Spinazzi, M., Casarin, A., Pertegato, V., Salviati, L., and Angelini, C. 2012. Assessment of mitochondrial respiratory chain enzymatic activities on tissues and cultured cells. *Nat Protoc* 7:1235-1246.

Supplemental Figure 1

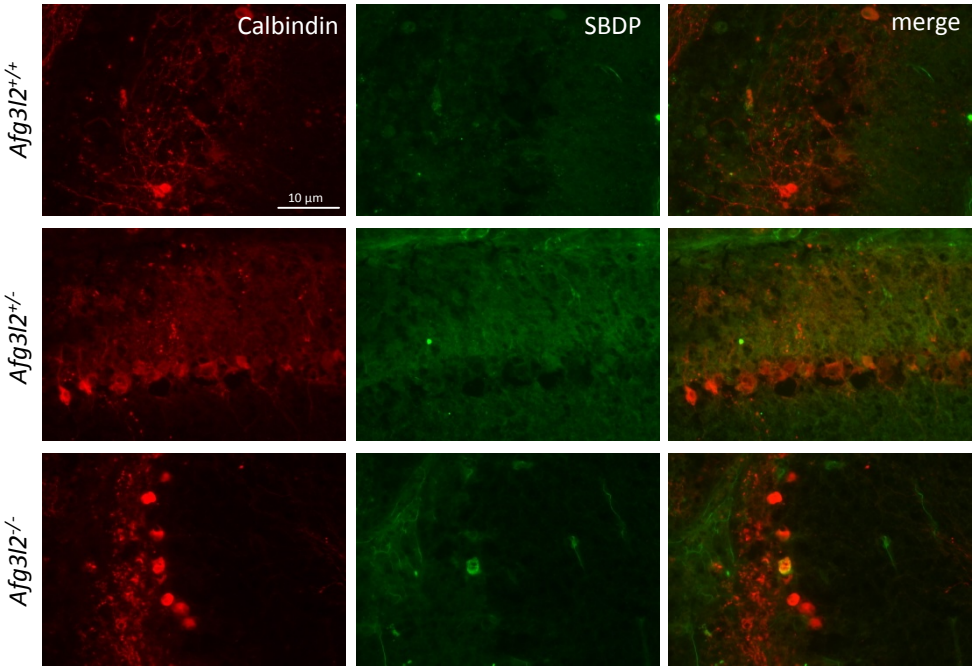

Supplemental Figure 2

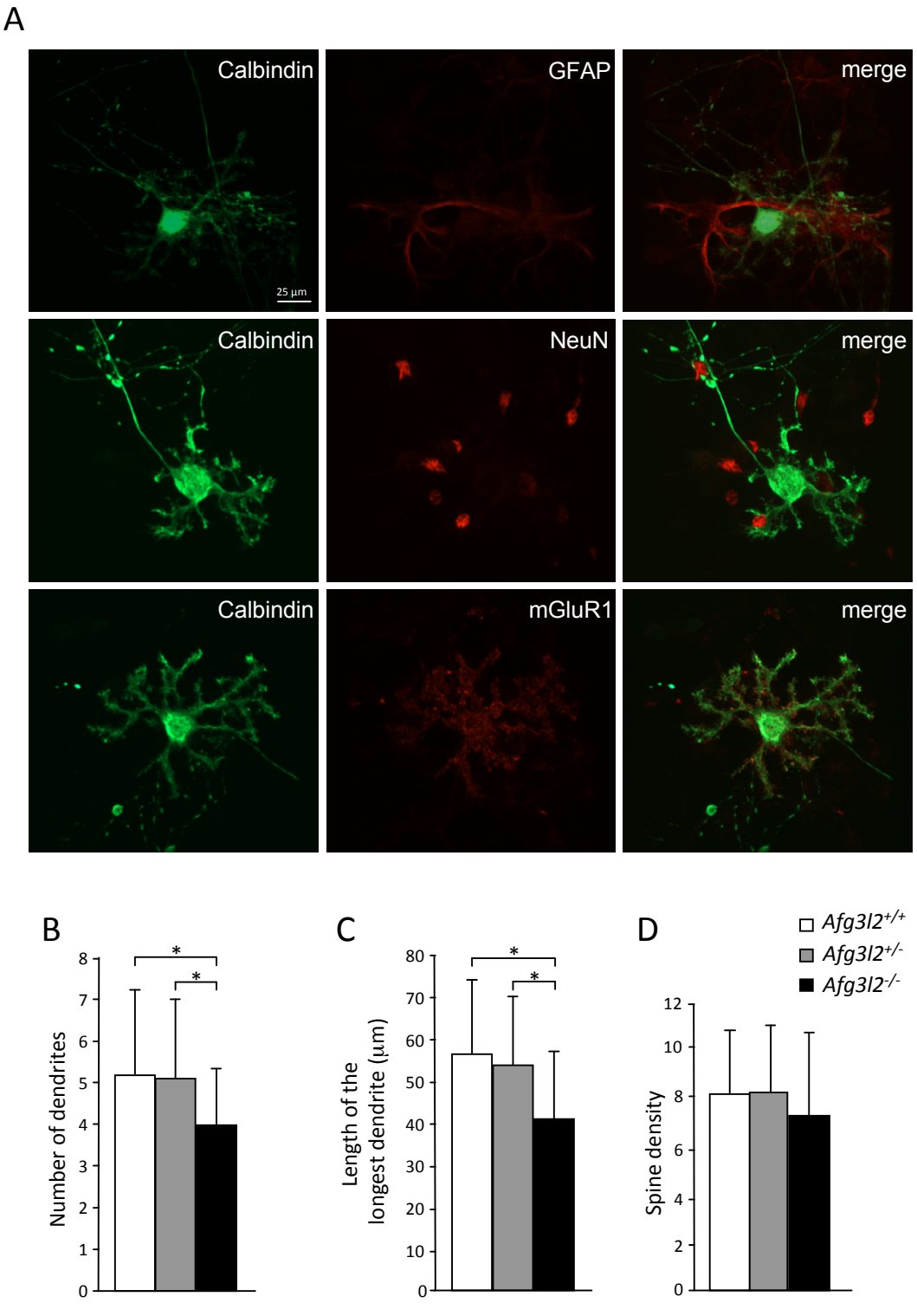

Supplemental Figure 3

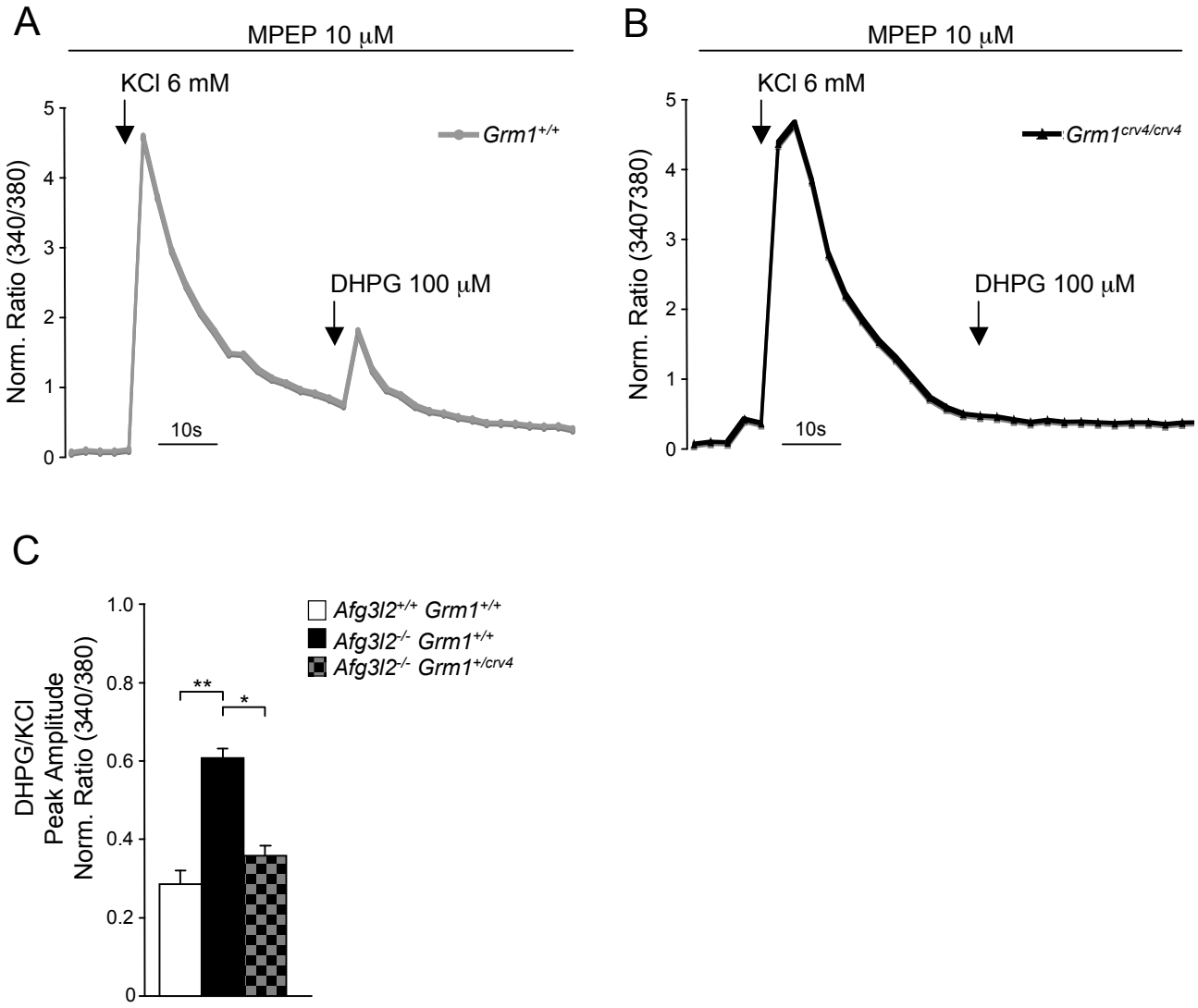

Supplemental Figure 4

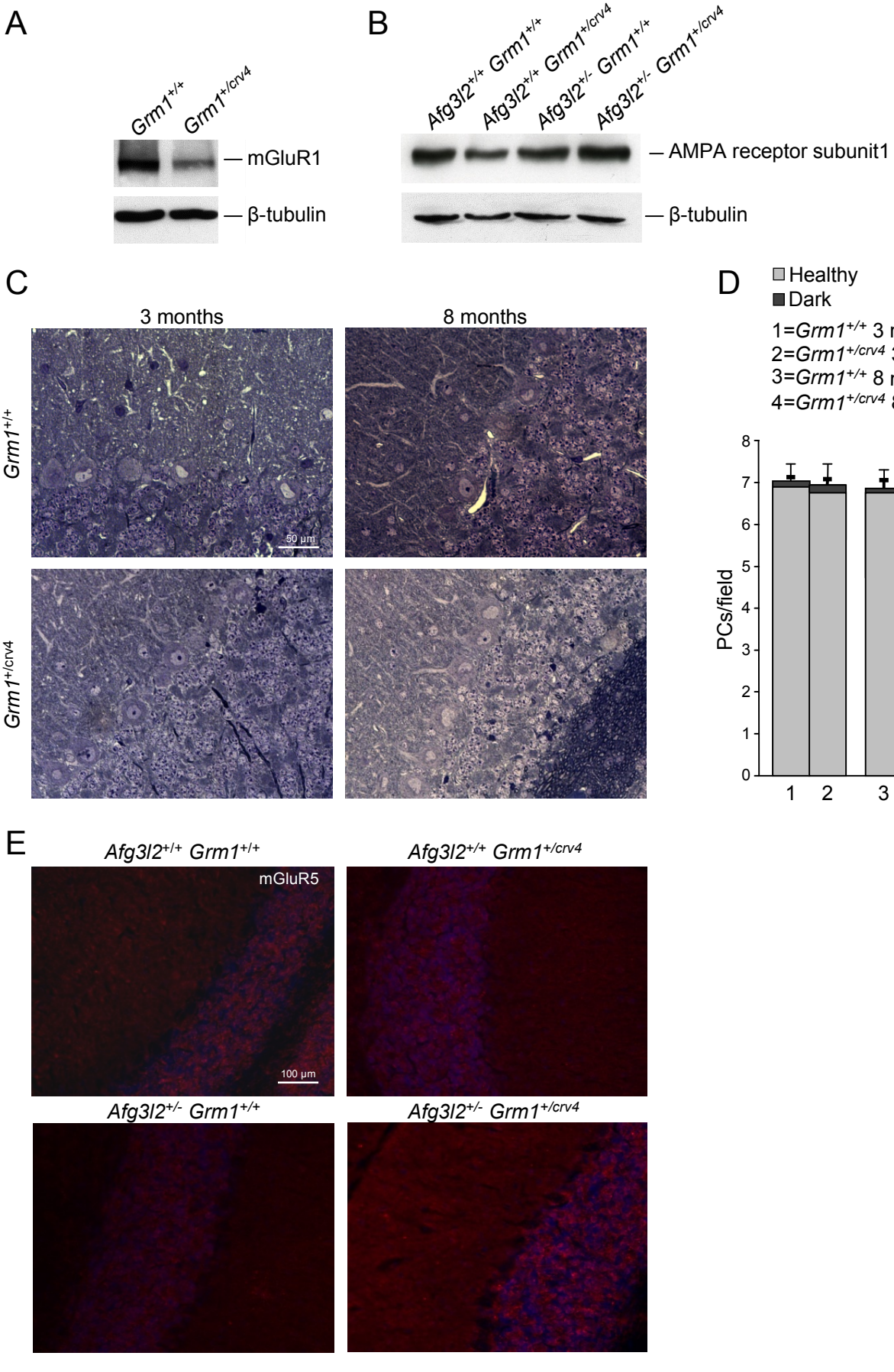

Supplemental Figure 5

A

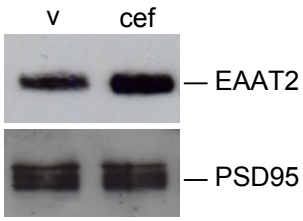

B

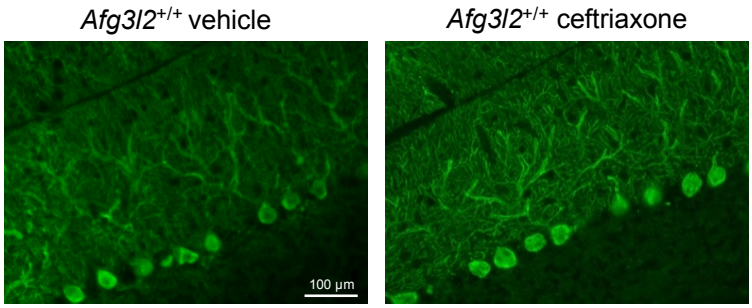

Supplemental Figure 6

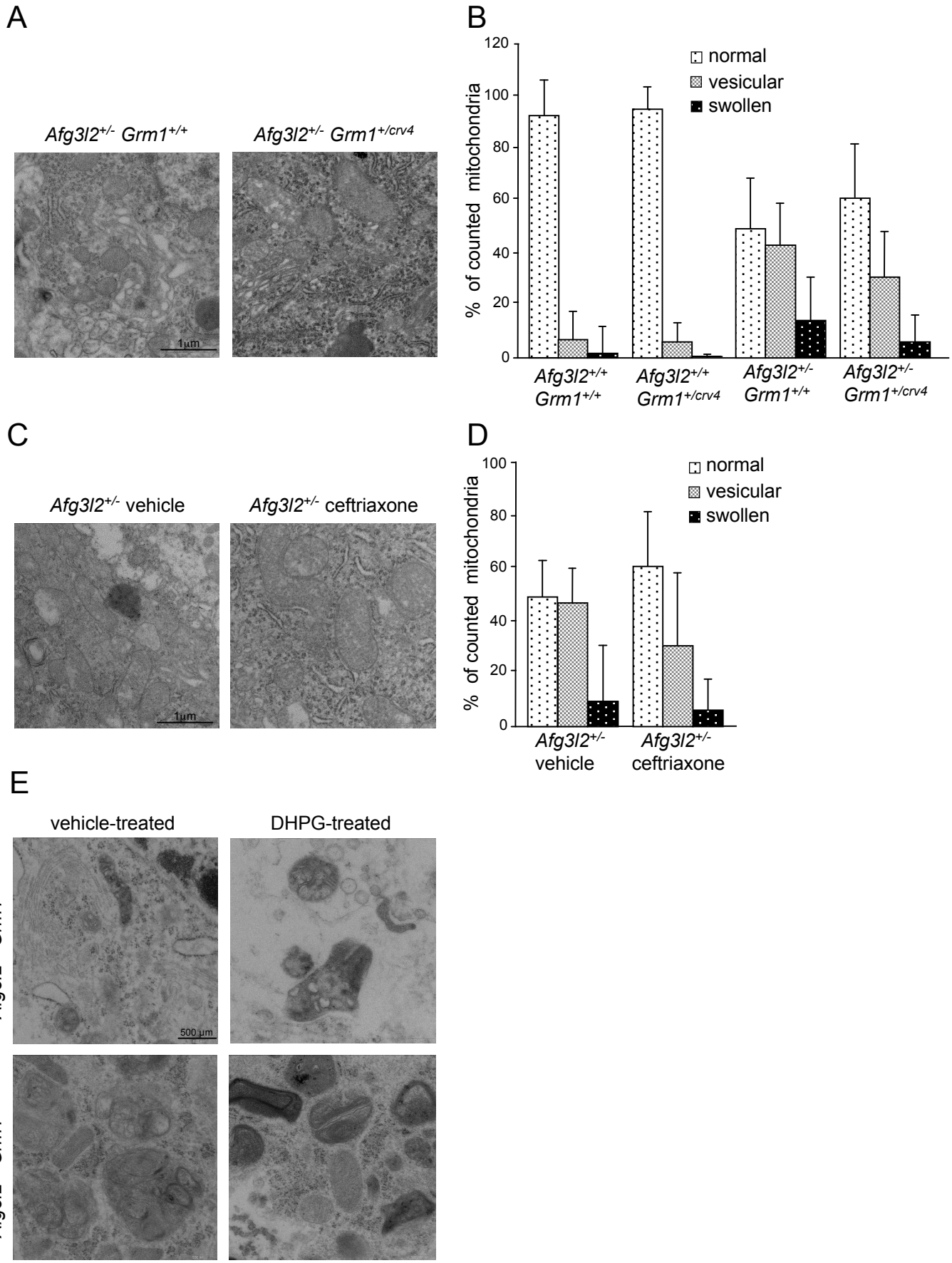

Supplemental Figure 7

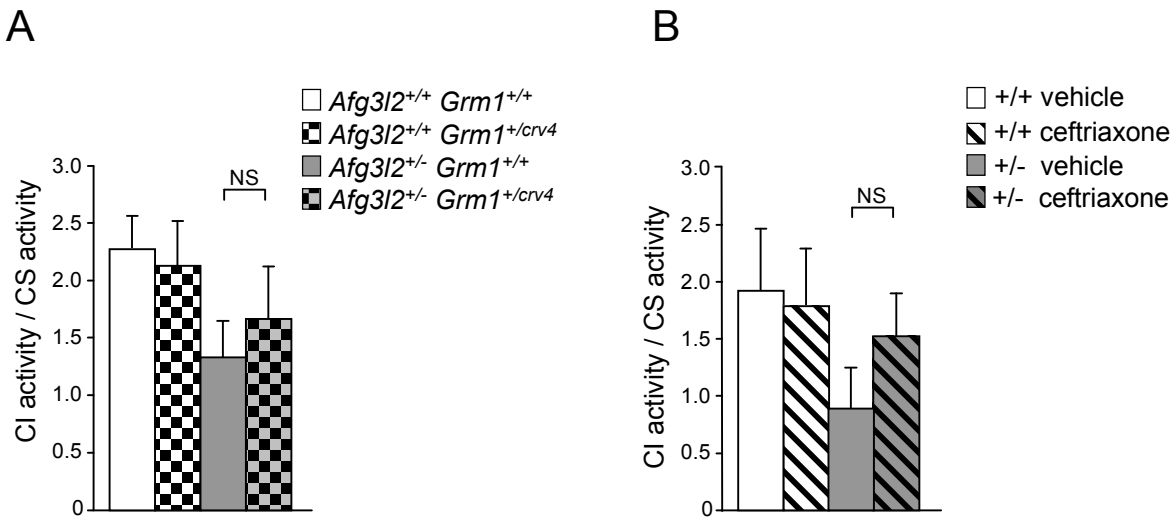

Supplemental Figure 8